An effective heterogeneous WO_3/TiO_2–SiO_2 catalyst for selective oxidation of cyclopentene to glutaraldehyde by H_2O_2

Ronghua Jin [a], Xin Xia [a], Weilin Dai [a], Jing-Fa Deng [a,*] and Hexing Li [b]

[a] *Department of Chemistry, Fudan University, Shanghai 200433, PR China*
E-mail: jfdeng@srcap.stc.sh.cn
[b] *Department of Chemistry, Shanghai Normal University, Shanghai 200234, PR China*

Received 7 May 1999; accepted 5 August 1999

TiO_2–SiO_2 mixed oxide with large pore size was synthesized by the xerogel method and it was then used to prepare the WO_3/TiO_2–SiO_2 catalyst by an incipient wetness method. The as-prepared WO_3/TiO_2–SiO_2 sample was employed as the first heterogeneous catalyst in the liquid-phase cyclopentene oxidation by aqueous H_2O_2, which exhibited higher selectivity (about 75%) to glutaraldehyde (GA) and, in turn, higher GA yield than the WO_3/SiO_2 heterogeneous catalyst and even the tungstic acid homogeneous catalyst under the same reaction conditions. The amorphous WO_3 phase was identified as the active sites and the loss of the active sites was proved to be not important. The lifetime of the catalyst was determined and its regeneration method was proposed. The effects of various factors on the catalytic behaviors, such as the WO_3 loading, the calcination temperature, the surface acidity and the reaction media, were investigated and discussed based on various characterizations including BET, XRD, XPS, FTIR, EXAFS and Raman spectra etc.

Keywords: catalytic oxidation, cyclopentene, H_2O_2, glutaraldehyde (GA), TiO_2–SiO_2 xerogel, WO_3/TiO_2–SiO_2 catalyst

1. Introduction

WO_3-based catalysts are important not only in the selective reduction of NH_3 [1–3] but also in the epoxidation of unsaturated compounds [4]. Supported tungsten oxide catalysts are very efficient for heterogeneous catalysis by various acids. However, almost no attention has been devoted to the use of these catalysts for the oxidative cleavage of carbon–carbon double bonds with aqueous H_2O_2 to produce dialdehydes, which are now mainly prepared by ozonization of olefins [5,6] or other synthetic methods [7,8]. Glutaraldehyde (GA) has been used extensively for disinfection and sterilization in many areas and has earned a justified reputation as an efficient chemosterilizer after being used for many years [9]. An important way to produce GA is the selective oxidative cleavage of cyclopentene, since a great quantity of cyclopentene could be easily obtained from the by-products of the C_5 fraction presented in refining oils [10,11]. Recently, several W-containing homogeneous catalysts have been reported which allowed the use of the environmentally friendly aqueous H_2O_2 as the oxidant for the cyclopentene selective oxidation to GA [12–14]. Although a high GA yield was obtained, their application in industrial processes seems almost impractical since these homogeneous catalysts are not easily separated from the reaction products and recovered. One of the most promising ways is to design heterogeneous catalysts. However, no such work has been reported so far, possibly owing to the poor catalytic efficiency of those heterogeneous catalysts. To our knowledge, it seems that the pore size of the support plays a key role in determining the catalytic activity since a large pore size of the support is necessary to ensure the oxidation of bulky cycloalkenes over those catalysts. In the present paper, we report a novel WO_3-based heterogeneous catalyst deposited on TiO_2–SiO_2 mixed oxide with larger pore size synthesized by the xerogel method. The as-prepared catalyst exhibited much higher selectivity to GA and higher GA yield than the WO_3/SiO_2 heterogeneous catalysts [15] and even the tungstic acid homogeneous catalyst in the liquid-phase cyclopentene oxidation by aqueous H_2O_2. The effects of various factors on its catalytic behaviors were determined and discussed according to various characterizations.

2. Experimental

2.1. Catalysts preparation

The titania–silica mixed oxide xerogel support was prepared by an alkoxide sol–gel method [16–18]. In general, the sol–gel procedures were carried out in a round-bottomed flask with a magnetic stirrer. Solution A was prepared by adding a hydrolysant comprised of certain amount of twice-distilled water and 36 wt% HCl in 30 ml ethanol to 40 ml ethanol solution containing 0.3 mol tetraethylorthosilicate (TEOS), leading to a hydrolysis level of 2 at 333 K for 1 h. Solution B was prepared by refluxing a solution containing 10 ml acetone, 10 ml ethanol and certain amount of tetrabutylorthotitanate (TBOT) at 333 K for 1 h under vigorous stirring. After solution B had been cooled down to ambient temperature, it was added to solution A under vigorous

* To whom correspondence should be addressed.

stirring. Then the additional hydrolysant in 100 ml ethanol was added and the solution was kept at 333 K, in which the molar ratio between H_2O : alkoxide : HCl was adjusted to be 5 : 1 : 0.1 to ensure that the rate of hydrolysis of Ti alkoxide could match that of Si alkoxide in the solution [19]. After drying at 353 K for 24 h and then calcining at 373 K for another 24 h, the resulting TiO_2–SiO_2 xerogel containing 2.5 wt% TiO_2 was then ground with mortar and pestle and sieved to 80–100 meshes. In the preparation of the supported WO_3 catalysts, the as-prepared TiO_2–SiO_2 xerogel support was impregnated with an aqueous solution of ammonium tungstate, $(NH_4)_2WO_4$, by an incipient wetness method at room temperature [2,20–22], dried at 378 K for 20 h in air, and calcined at 823 K for another 12 h. For comparison, the WO_3/SiO_2 catalyst was also prepared by the incipient wetness method, as described above. $WO_3{\cdot}H_2O$ was available commercially. The bulk WO_3 was prepared by treating the $WO_3{\cdot}H_2O$ sample at 673 K for 12 h. Unlike the $WO_3{\cdot}H_2O$ sample, the resulted anhydrous WO_3 was found to be insoluble in the aqueous H_2O_2 solution.

2.2. Catalyst characterization

Specific surface areas (BET) and mean cylindrical pore diameters were determined by nitrogen physisorption at 77 K using a Micromeritics ASAP 2000 instrument.

X-ray powder diffraction (XRD) patterns were obtained on a Bruker D8 Advance X-ray generator using Cu Kα radiation ($\lambda = 1.54$ Å) at 40 kV and 40 mA.

X-ray photoelectron spectra (XPS) measurements were performed on a Perkin–Elmer PHI 5000C ESCA system with standard Al Kα radiation (1486.6 eV) at 93.90 eV pass energy and low magnification. The base pressure of the test chamber was 1×10^{-9} Torr.

Extended X-ray absorption fine structure (EXAFS) was performed. The absorption data of the W K edge were collected at the 4W1B beamline at the Beijing Synchrotron Radiation Facility, China. The electron beam energy is 22.0 GeV and the stored current is in the range of 30–50 mA. The monochromator is a channel-cut Si(111) crystal monochromator, $d = 0.31355$ nm. The data were collected in the transmission mode using ion chambers of nitrogen (75%)/argon (25%) mixed gas at room temperature from 8050 to 9400 eV. We registered data three times for estimating the deviation. Data were processed by using the program package FXEA.

Raman spectra were recorded with a Superlab Ram Raman spectrometer with a resolution of 2 cm^{-1}. The laser power at the sample location was set to 15 mW. The excitation line of the Raman scattering was 632.817 nm.

2.3. Activity test

In a typical run, the oxidation experiment was carried out in a sealed 50 ml reactor in which 34 mmol of cyclopentene (Fluka), 30 ml of t-BuOH as the solvent, and 1.0 g catalyst were mixed at 308 K. Then, 60 mmol of 50% aqueous H_2O_2 solution (Industrial grade) was added via a dropping funnel under vigorous stirring and was allowed to react for 20 h. The conversion of cyclopentene was measured by a gas chromatograph (TCD) using cyclopentane as an internal standard. The yield of GA was measured by a gas chromatograph (FID) using an external standard method. The products were determined by GC-MS. The H_2O_2 was measured by standard iodometric titration.

3. Results and discussion

3.1. Structural characteristics of the catalysts

The XRD patterns, as shown in figure 1, revealed that the bulk WO_3 was present in a fine crystalline structure, while both the TiO_2–SiO_2 and the WO_3/TiO_2–SiO_2 samples were in the amorphous states. During the reaction, the WO_3/TiO_2–SiO_2 catalyst gradually crystallized accompanied by a decrease in activity. However, the amorphous state of the catalyst could be recovered by treating the deactivated sample at 823 K for 6 h. Unfortunately, the regeneration mechanism was still not very clear now. The effect of the calcination temperature on the structure of the WO_3/TiO_2–SiO_2 catalyst was investigated by an *in situ* XRD technique at elevated temperature from 473 to 1073 K. As shown in figure 2, the WO_3/TiO_2–SiO_2 sample was present in the amorphous state at the calcination temperature $<$823 K. However, when calcination temperature was further increased from 823 to 1073 K, several diffraction peaks corresponding to the crystalline WO_3 phases were observed, indicating the occurrence of crystallization at high temperature.

The Raman spectra provided additional information about the structure of the TiO_2–SiO_2 xerogel support and WO_3/TiO_2–SiO_2 samples at calcination temperatures of 823 and 1073 K, respectively. From figure 3 one can see that the WO_3/TiO_2–SiO_2 calcined at 823 K was present in a totally amorphous state since no significant peaks appeared.

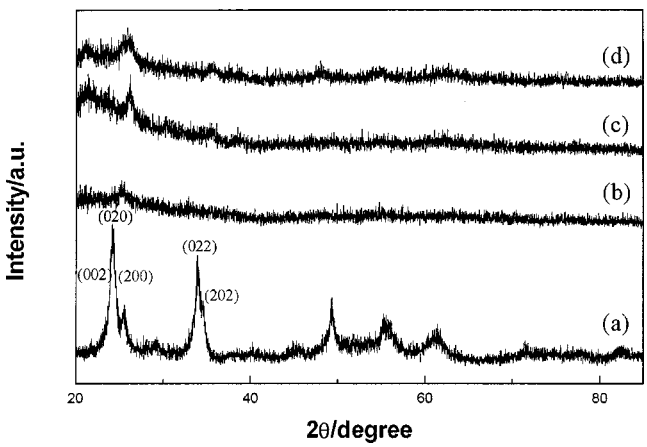

Figure 1. XRD diagrams of (a) bulk WO_3, (b) 2.5% TiO_2–SiO_2, (c) 15%WO_3/TiO_2–SiO_2 calcined at 823 K, (d) 15%WO_3/TiO_2–SiO_2 after regeneration at 823 K for 6 h.

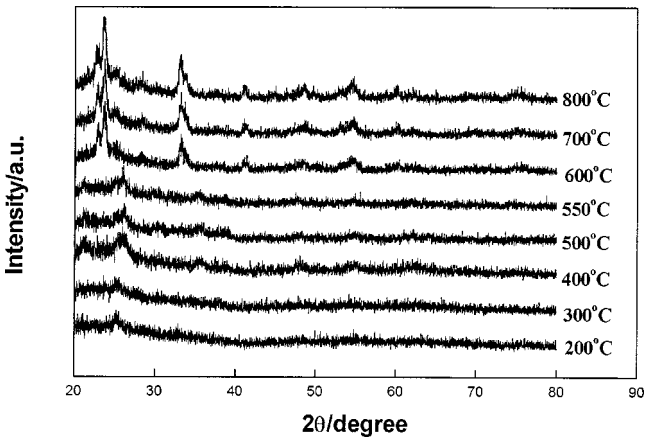

Figure 2. *In situ* XRD diagrams of 15 wt% WO_3/TiO_2–SiO_2 sample calcined at elevated temperature from 473 to 1073 K.

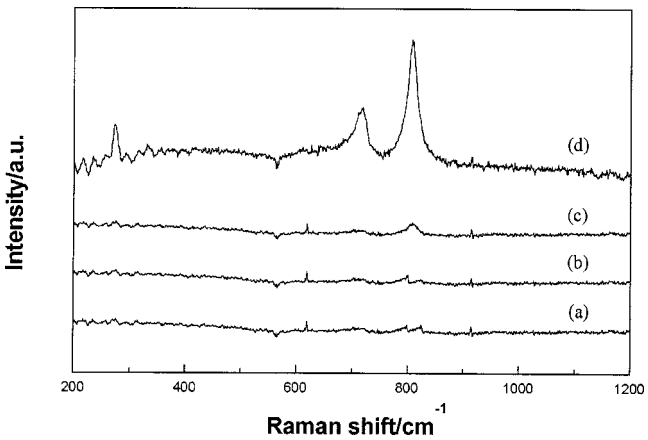

Figure 3. Raman spectra of sample (a) TiO_2–SiO_2 calcined at 823 K, (b) TiO_2–SiO_2 calcined at 1073 K, (c) 15%WO_3/TiO_2–SiO_2 calcined at 823 K, (d) 15%WO_3/TiO_2–SiO_2 calcined at 1073 K.

It was also found that no significant peaks appeared for the TiO_2–SiO_2 support even if it was treated at 1073 K. Therefore, it was concluded that both the bulk WO_3 and the WO_3/TiO_2–SiO_2 calcined at 1073 K were in the crystalline state since various strong bands at around 800, 720 and 270 cm^{-1} were observed similar to those observed in the well crystalline WO_3 samples [23,24], which were assigned to the symmetric stretching mode of W–O, bending mode of W–O and the deformation mode of W–O–W, respectively.

The RDF curves of the bulk WO_3 and WO_3/TiO_2–SiO_2 samples obtained from Fourier transforms of their EXAFS $k^2\chi$ at the W L_3 edge are shown in figure 4. The peaks between $R = 0.6$ and 2.5 Å are assigned to W–O bonds and the peaks at $R = 3.7$ Å to the W–W bonds [25]. In comparison with that of bulk WO_3, the RDF curve of the WO_3/TiO_2–SiO_2 sample shows a new peak at 3.3 Å, possibly attributed to a W–Si bond resulting from WO_3 anchoring onto the TiO_2–SiO_2 surface. A new peak at 2.1 Å with a high Debye–Waller factor was presumably corresponding to the W–O bonds in the W–O–W and W–O–Si or W–O–Ti bridges [26], as confirmed by Raman spectra [27]. The

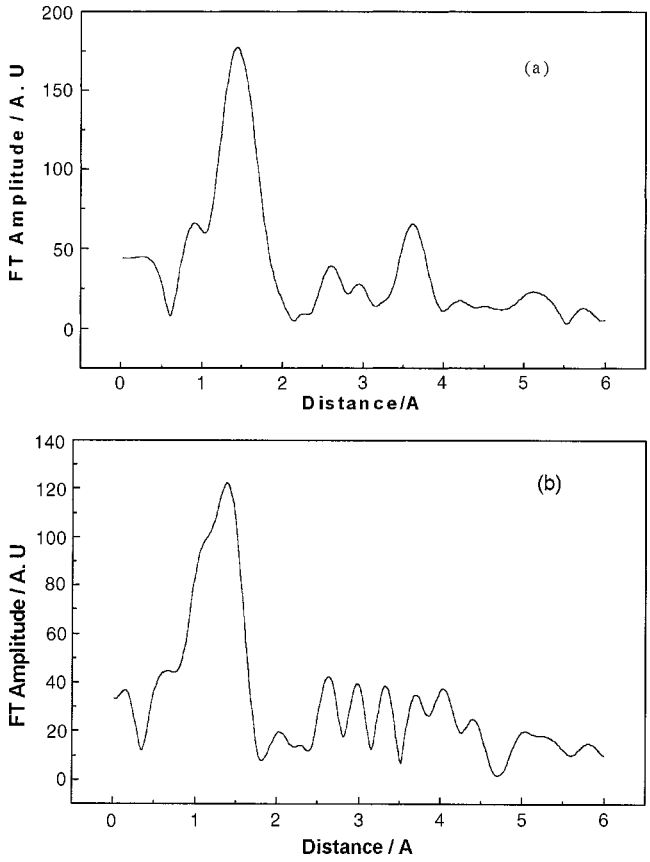

Figure 4. RDF curves of W K edge in (a) bulk WO_3, (b) 15%WO_3/TiO_2–SiO_2 sample.

calculation from the EXAFS data also revealed that the coordination number of W in the above-mentioned bridges was 4.8, much smaller than that of W in bulk WO_3, showing that the W centers on the surface were highly unsaturated [23].

Other structural properties, such as the BET surface area, the pore volume and the mean cylindrical pore diameters of various samples are summarized in table 1.

3.2. Performance of different catalysts

The catalytic behaviors of various catalysts are listed in table 1. One can see that SiO_2 is totally inert while both TS-2 and TiO_2–SiO_2 xerogel exhibited some activity for epoxidation of cyclopentene to cyclopentene oxide (CPO). The activity of TS-2 was much poorer than that of the as-prepared TiO_2–SiO_2 xerogel, possibly owing to its small pore size [28,29]. In comparison with different WO_3-based catalysts, the following results could be obtained from table 1:

(1) Although the cyclopentene conversion over the WO_3/TiO_2–SiO_2 xerogel catalyst was slightly less than that with the W-containing homogeneous catalyst obtained by dissolving $WO_3 \cdot H_2O$ in the reaction solution, the as-prepared heterogeneous catalyst exhibited much higher selectivity to GA and, in turn, a bit higher GA yield than its corresponding homogeneous catalyst. This is of great in-

Table 1
Oxidation of cyclopentene (CP) by H_2O_2 over different catalysts.[a]

Catalyst	BET ($m^2\,g^{-1}$)	V_p (N_2) ($m^2\,g^{-1}$)	d_p (nm)	Conversion (%)		Selectivity (%)	
				CP	H_2O_2	GA	CPO[b]
SiO_2	634	0.9	2.4	0	0	0	0
TS-2	487	0.5	0.55	4.0	8.6	0.9	3.7
TiO_2–SiO_2[c]	739	0.9	2.3	73.5	43.1	0.9	95.5
$WO_3{\cdot}H_2O$[d]	–	–	–	100	100	62.3	0.7
WO_3[e]	–	–	–	1.5	0.1	0	0
WO_3/SiO_2	522	0.5	2.1	98.8	100	58.9	0.5
WO_3/TiO_2–SiO_2[f]	622	0.5	2.0	84.7	100	75.2	0.5
WO_3/TiO_2–SiO_2[g]	608	0.5	2.0	84.2	99.5	75.0	0.6

[a] Reaction conditions: 308 K, 1.0 g catalyst, 34 mmol CP, 60 mmol 50% H_2O_2, 30 ml *t*-BuOH, reaction for 20 h.
[b] CPO = cyclopentene oxide.
[c] 2.5 wt% TiO_2 in the TiO_2–SiO_2.
[d] Homogeneous catalyst.
[e] Insoluble WO_3 obtained after $WO_3{\cdot}H_2O$ was calcined at 673 K.
[f] 15 wt% WO_3 loading.
[g] Regenerated at 823 K.

dustrial importance owing to its higher catalytic efficiency, less by-products, easier separation from the reaction product, longer lifetime and more convenient regeneration procedure.

To make sure whether the heterogeneous WO_3 on the TiO_2–SiO_2 support or the dissolved homogeneous WO_3 was the real catalyst responsible for the present oxidation [30], the following procedure was carried out. On the one hand, the loss of the active sites during the cyclopentene oxidation over 15 wt% WO_3/TiO_2–SiO_2 (calcination temperature = 823 K) was analyzed by ICP. Only 7.4 ppm WO_3 species were determined in the solution after the reaction for 20 h, indicating the loss of the active sites could be neglected. On the other hand, after reaction for 4 h in which the cyclopentene conversion reached nearly 50%, the reaction mixture was filtered and then the mother liquor (filtrate) was allowed to react for another 16 h under the same reaction conditions. No significant activity was observed, demonstrating that the active species are not the dissolved WO_3 leached from WO_3/TiO_2–SiO_2. Therefore, it is clear that the present catalysis is heterogeneous in nature.

(2) The WO_3/TiO_2–SiO_2 xerogel catalyst exhibited much better selectivity to GA and, in turn, a higher GA yield than the corresponding WO_3/SiO_2 xerogel prepared by the same method. This could be understood by considering the reaction pathway and the role of the TiO_2–SiO_2 xerogel in the reaction. According to the GC-MS analysis, besides GA as the main product, a variety of by-products, such as cyclopentene oxide (CPO), *trans*-1,2-cyclopentanediol and its monoether as well as a trace of cyclopentanone and 2-cyclopenten-1-one were identified, indicating that the reaction was very complex in which different oxidation routes and even the hydrolysis of CPO possibly occurred. Over the 15 wt% WO_3/TiO_2–SiO_2 xerogel catalyst, the dependence of the consumption of cyclopentene and the formation of GA and various by-products on the reaction time was determined, as shown in figure 5. One can see that CPO was produced rapidly at the beginning and

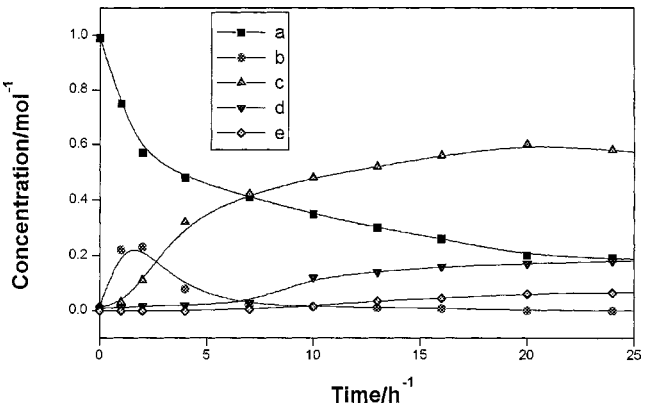

Figure 5. Production of the oxidation from by the WO_3/TiO_2–SiO_2 xerogel catalyst: (a) cyclopentene, (b) cyclopentene oxide, (c) glutaraldehyde, (d) *trans*-1,2-cyclopentanediol, (e) 1,2-cyclopentanediol monoether.

then consumed progressively with the increase of GA, indicating that CPO was possibly a main intermediate from which GA was produced via its further oxidative cleavage. This could satisfactorily account for the better selectivity to GA over WO_3/TiO_2–SiO_2 than over WO_3/SiO_2, since TiO_2–SiO_2 xerogel exhibited excellent activity for producing CPO.

According to the FTIR spectra of pyridine adsorption, there were 2.5×10^{18} active sites of B acid and 1.1×10^{18} active sites of Lewis acid in each gram of the WO_3/TiO_2–SiO_2 catalyst, while no significant surface acidic sites were determined in WO_3/SiO_2. Therefore, the higher selectivity of WO_3/TiO_2–SiO_2 to GA than that of WO_3/SiO_2 could also be partially attributed to the promoting effect of its surface acidity. This was confirmed by the fact that the WO_3/TiO_2–SiO_2 catalyst doped with trace of a strong acid slightly increased its selectivity to GA, while doping the catalyst with Na^+ or K^+ greatly reduced its selectivity to GA.

(3) After reaction for three times, a significant decrease in the activity and selectivity of the WO_3/TiO_2–SiO_2 catalyst was observed. Such a deactivated catalyst was almost completely regenerated after it was calcined at 823 K for

6 h. These results suggested that only the amorphous WO_3 phases could serve as the active sites in the present reaction since the catalyst gradually crystallized during the reaction and the amorphous state could be recovered after the deactivated catalyst was regenerated, as shown in figure 1. Almost no activity was observed over the bulk WO_3, which could be considered as a heterogeneous WO_3 catalyst since it is insoluble in the aqueous H_2O_2. This also supported the above assumption that the active sites of WO_3/TiO_2–SiO_2 catalyst were amorphous WO_3 phases since the bulk WO_3 was present in a well crystalline state.

The higher activity of the amorphous WO_3 phases than that of its corresponding crystalline phases could be understood by considering the differences between structural properties, as mentioned above. On the one hand, the RDF curves and the Raman spectra revealed the presence of W–O–Si or W–O–Ti bridges in the amorphous WO_3/TiO_2–SiO_2 catalyst, which have been proved to be favorable for the selective oxidation reaction [31–34]. On the other hand, according to the calculation from the EXAFS data, the coordination number of W in the amorphous WO_3/TiO_2–SiO_2 catalyst was much lower than that in either the crystalline WO_3/TiO_2–SiO_2 catalyst obtained by calcination at 1073 K or the bulk WO_3 (well crystallized sample), indicating that the W species in the amorphous WO_3/TiO_2–SiO_2 catalyst was more highly unsaturated. As is well known, the highly unsaturated active sites were also favorable for the adsorption of the reactants, which in turn resulted in the higher activity in the present reaction [35,36].

3.3. Influence of the calcination temperature

The effect of the calcination temperature on the catalytic behaviors of a WO_3/TiO_2–SiO_2 catalyst with 15 wt% WO_3 loading is shown in table 2. One can see that the catalyst retained its high activity and selectivity to GA at the calcination temperature <823 K. However, both the activity and selectivity decreased abruptly when the calcination temperature increased from 823 to 1073 K. Those results could also be explained based on the above assumption since no significant crystallization was observed at the calcination temperature <823 K, while the catalyst gradually crystallized with the increase of calcination temperature from 823 to 1073 K, as shown in figure 2. The 823 K was chosen as the optimum calcination temperature for the 15 wt% WO_3/TiO_2–SiO_2 catalyst because at that temperature the leaching of the active WO_3 was effectively inhibited while no significant crystallization occurred. It should be noted that the optimum calcination temperature changed with the WO_3 loading. Lower calcination temperature should be employed with the increase of WO_3 loading, as discussed in section 3.4.

Table 2
Influence of the calcination temperature on the performance of WO_3/TiO_2–SiO_2 catalyst with 15 wt% WO_3 loading.[a]

Temperature (K)	Conversion (%)		Selectivity of GA (%)	Leaching of WO_3 (ppm)
	CP	H_2O_2		
673	92.2	61.5	59.1	101
723	90.6	82.9	62.7	82
773	86.3	100	68.5	15.5
823	84.7	100	75.2	7.4
873	24.5	30.7	27.3	0.5
1073	6.3	3.9	20.1	0

[a] Reaction conditions are as the same as given in table 1.

3.4. Influence of WO_3 loading

The effect of the WO_3 loading on the performance of the WO_3/TiO_2–SiO_2 catalyst is shown in table 3. Both the activity and selectivity increased with the increase of the WO_3 loading up to 20 wt%, while the further increase of the WO_3 loading resulted in the decrease in its activity. The XRD patterns show that, at lower WO_3 loading (<20 wt%), the WO_3 species were well dispersed on the support surface without significant crystallization. However, at WO_3 loading >20 wt%, partial crystallization occurred due to the gathering of the WO_3 species. Therefore, the promoting effect of WO_3 loading (when it was less than 20 wt%) was mainly attributed to its effect on the number of surface active WO_3 sites, since the surface W/Si ratio increases almost linearly with the WO_3 loading up to ~20%, as determined by XPS spectra (see figure 6). However, at WO_3 loading >20 wt%, no significant increase in surface W/Si ratio was observed. In contrast, as discussed above, the crystalline WO_3 appeared at higher WO_3 loading, responsible for the decrease in its activity.

Table 3
Influence of WO_3 loading on the performance of WO_3/TiO_2–SiO_2 catalyst.[a]

WO_3 loading (wt%)	Conversion (%)		Selectivity to GA (%)
	CP	H_2O_2	
5	27.5	35.6	62.1
10	59.7	67.3	67.4
15	84.7	100	75.2
20	86.2	100	72.9
25	57.8	70.2	72.3

[a] Reaction conditions are as the same as given in table 1.

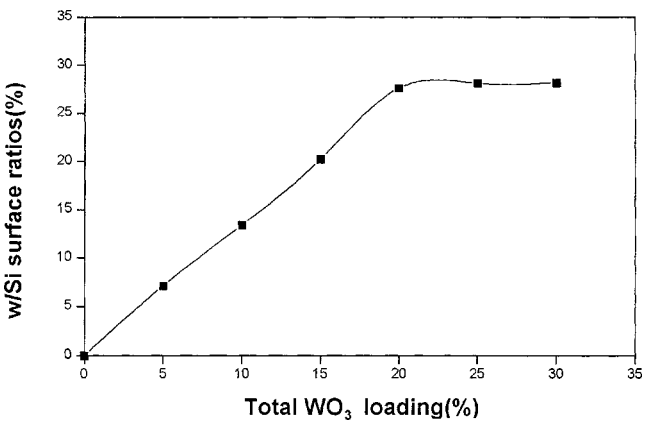

Figure 6. XPS surface ratio W/Si versus total WO_3 loading (wt%).

Table 4
Influence of the solvent on the performance of WO_3/TiO_2–SiO_2 catalyst with 15 wt% WO_3 loading.[a]

Solvent	Conversion of CP (%)	Selectivity of GA (%)
MeOH	94.2	12.8
EtOH	90.5	42.5
i-PrOH	84.4	68.0
t-BuOH	84.7	75.2
MeCN	72.7	61.1
THF	76.1	61.9

[a] Reaction conditions: 30 ml each of the solvents. Other conditions are as the same as given in table 1.

3.5. Effect of the solvents

It is well known that the solvent plays a very important role in determining the catalytic activity and selectivity in many catalytic oxidations by H_2O_2 [37]. The effect of various solvents on the catalytic behaviors of the WO_3/TiO_2–SiO_2 catalyst in the present reaction is listed in table 4. In the *tert*-butanol (*t*-BuOH) medium, the catalyst exhibited higher conversion and better selectivity to GA than in other media except for MeOH and EtOH, such as isopropanol (*i*-PrOH), acetonitrile (MeCN) and tetrahydrofuran (THF). This could be possibly attributed to the reaction between H_2O_2 and *t*-BuOH with WO_3/TiO_2–SiO_2 as an acid catalyst, yielding *tert*-butyl hydroperoxide (TBHP) as determined by GC-MS analysis, which has been proved to be an excellent oxidant for the selective cyclopentene oxidation to GA in liquid phase. Another reason may be that *t*-BuOH is a good solvent for both the reactants and the reaction products. Although high conversion could be obtained in methanol (MeOH) or ethanol (EtOH) media, both of them could not be employed in the present reaction because of the very poor selectivity to GA. Its was also found that both MeOH and EtOH could be partially oxidized during the reaction, while the *t*-BuOH can be regenerated from TBHP after it reacted with cyclopentene. Therefore, the *t*-BuOH was determined as the optimum solvent in the present reaction.

4. Conclusion

The following conclusions can be drown from this study:

(1) The WO_3/SiO_2–TiO_2 catalyst is one of the powerful heterogeneous catalysts for the liquid-phase cyclopentene oxidation by H_2O_2, due to its high selectivity and yield to GA and the easy procedure for separating it from the reaction product and for its regeneration.

(2) In the WO_3/SiO_2–TiO_2 catalyst, the amorphous WO_3 is determined as the active sites. The optimum calcination temperature is determined as 823 K and the optimum WO_3 loading is determined as 15 wt%. From various solvents, *t*-BuOH seems to be the best one in the present oxidation reaction.

(3) The SiO_2–TiO_2 mixed oxide plays a promoting effect on the GA yield in the present reaction, which results in the higher selectivity to GA and GA yield over the WO_3/SiO_2–TiO_2 catalyst than those over the corresponding WO_3/SiO_2 catalyst.

Finally, various characterizations have been employed to elucidate the correlation of the catalytic behaviors of the WO_3/SiO_2–TiO_2 catalyst to its structural properties. However, it should be noted that further studies are required in order to understand fully the micromechanism of the present oxidation reaction and the roles of the WO_3/SiO_2–TiO_2 catalyst. Those works are being underway.

Acknowledgement

This work was supported by the SINOPEC.

References

[1] S. Morikawa, K. Takahashi, J. Mogi and S. Kurita, Bull. Chem. Soc. Jpn. 55 (1982) 2254.
[2] C. Martin, G. Solana, V. Rives, G. Marci, L. Palmisano and A. Sclafani, Catal. Lett. 49 (1997) 235.
[3] H. Kamata, K. Takahashi and C.U.I. Odenbrand, Catal. Lett. 53 (1998) 65.
[4] Z. Zhang, J. Suo, X. Zhang and S. Li, J. Chem. Soc. Chem. Commun. (1998) 241.
[5] Y. Ishii, K. Yamawaki, T. Ura, H. Yoshida and M. Ogawa, J. Org. Chem. 53 (1988) 3587.
[6] Oguchi, T. Ura, Y. Ishii and M. Ogawa, Chem. Lett. (1989) 857.
[7] G.M. Karagezyan et al., USSR SU 878760 (1981).
[8] Daicel Chemical Industries Ltd. Co., JP 59108734 (1984).
[9] S.P. Gorman, E.M. Scott and A.D. Russell, J. Appl. Bacteriol. 48 (1980) 161.
[10] W.J. Wang, M.H. Qiao, H.X. Li and J.-F. Deng, Appl. Catal. A 166 (1998) 243.
[11] W.J. Wang, M.H. Qiao, H.X. Li, W.L. Dai and J.-F. Deng, Appl. Catal. A 168 (1998) 151.
[12] H. Furakawa, T. Nakamura, H. Inagaki, E. Nishikawa, C. Imai and M. Misono, Chem. Lett. (1988) 877.
[13] J.-F. Deng, X.H. Xu, H.Y. Chen and A.R. Jiang, Tetrahedron 48 (1992) 3503.
[14] K.-Y. Lee, K. Itoh, M. Hashimoto, N. Mizuno and M. Misono, Stud. Surf. Sci. Catal. 82 (1994) 583.
[15] R. Jin, X. Xia, D. Xue and J.-F. Deng, Chem. Lett. (1999) 371.
[16] B.E. Yoldas, J. Non-Cryst. Solids 38 (1980) 81.
[17] M. Aizawa, Y. Nosaka and N. Fujii, J. Non-Cryst. Solids 128 (1991) 77.
[18] D.C.M. Dutoit, M. Schneider and A. Baiker, J. Catal. 153 (1995) 165.
[19] A. Thangaraj, R. Kumar, S.P. Mirajkar and P. Ratnasamy, J. Catal. 130 (1991) 1.
[20] K. Arata, Adv. Catal. 37 (1989) 165.
[21] W. Ji, J. Hu and Y. Chen, Catal. Lett. 53 (1998) 15.
[22] N. Vaidyaanathan, M. Houaua and D.M. Hercules, Catal. Lett. 43 (1997) 209.
[23] I.E. Wachs, F.D. Hardcastle and S.S. Chan, Spectroscopy 1 (1986) 30.
[24] M.A. Vuurman and I.E. Wachs, J. Phys. Chem. 95 (1991) 9928.
[25] E. Salje and H.M. Rietveld, Acta Crystallogr. A 31 (1975) 356.
[26] F. Hilbrig, H.E. Gobel, H. Knözinger, H. Schmelz and B. Lengeler, J. Phys. Chem. 95 (1991) 6973.

[27] I.E. Wachs, D.S. Kim and M. Ostromecki, J. Mol. Catal. A 106 (1996) 93.
[28] A. Corma, M.A. Camblor, P. Esteve, A. Martinez and J. Perez-Pariente, J. Catal. 145 (1994) 151.
[29] R. Hutter, T. Mallat and A. Baiker, J. Catal. 153 (1995) 177.
[30] R.A. Sheldon, M. Wallau, I.W.C.E. Arends and U. Schuchardt, Acc. Chem. Res. 31 (1998) 485.
[31] D.B. Dadyburjor, S.S. Jewur and E. Ruckenstein, Catal. Rev. Sci. Eng. 19 (1979) 293.
[32] J. Haber, in: *New Developments in Selective Oxidation by Heterogeneous Catalysis*, Vol. 72, ed. B. Delmon (Elsevier, Amsterdam, 1992) p. 279.
[33] H.H. Kung, Ind. Eng. Chem. Prod. Res. Dev. 25 (1986) 171.
[34] G. Centi and F. Trifirò, Appl. Catal. 12 (1984) 1.
[35] À. Molnár, G.V. Smith and M. Bartók, Adv. Catal. 36 (1989) 329.
[36] J.-F. Deng, J. Yang and S. Sheng, J. Catal. 150 (1994) 434.
[37] V. Hulea, E. Dumitriu, F. Patcas, R. Ropot, P. Graffin and P. Moreau, Appl. Catal. A 170 (1998) 169.